# Some Materials and Cooling Techniques Applicable to Air-Breathing Engines at High Flight Speeds

R. J. E. GLENNY* AND J. F. BARNES†
*National Gas Turbine Establishment, Pyestock, Hampshire, England*

**By drawing on experimental evidence, this paper indicates the extent to which both improved turbine blade materials and the use of internal cooling can permit increased turbine inlet temperatures during supersonic cruise, and can affect turbine design and engine performance. The limitations of nickel-based alloys and the prospects for more refractory materials are discussed. The extent to which internal cooling per se can allow increased gas temperatures and the effects on laboratory creep and fatigue properties of different methods of introducing cooling passages are described.**

## 1. Introduction

WORK at present in progress at the National Gas Turbine Establishment (NGTE) in the fields of high temperature materials and cooling techniques is aimed mainly at the high temperature (2880°R at inlet) gas turbine, which must become particularly important if reasonably low engine specific weights are to be achieved by flight Mach numbers between 2 and 3. This paper is concerned mainly with describing recent research at NGTE on turbine blade materials and cooling techniques.

## 2. Turbine Blade Materials

Further progress in aero-engine development depends on our ability to provide materials with a better retention of strength properties at higher temperatures and with an improved strength-weight ratio. In addition to these requirements, any new material must possess adequate resistance to fatigue, corrosion, and impact, i.e., adequate toughness. For materials that yield and exhibit plastic flow, the capacity for deformation must be sufficient to provide, for example, crack tolerance under cyclic loads or resistance to creep under steady loads. The greatest attention has been and still is being devoted to the development of materials that will perform at higher temperatures, because an increase in turbine inlet temperature is the most direct way of obtaining greater power output (and consequently reduced bulk and lower weight).

The quest for high temperature materials that will replace nickel- or cobalt-based alloys in critical components such as turbine blading has been in progress since the Second World War. Limited laboratory tests on materials such as cermets (ceramic/metal mixtures) and protected molybdenum alloys have encouraged and intensified the search; and although the interest in these particular materials has diminished considerably as a result of engine tests, these disappointments have not damped the enthusiasm of metallurgists, ceramists, and those contemporary materials engineers who, for want of a better word, might be called "compositeers." In the light of the activities of the NGTE, it is of interest to examine the merits, disadvantages, and prospects of current nickel-base alloys and of alternative materials for gas turbine rotor blading.

Presented at the AIAA/RAeS/JSASS Aircraft Design and Technology Meeting, November 15–18, 1965, Los Angeles, Calif.; submitted January 21, 1966; revision received June 7, 1966.

* Head, Materials Department.

† Turbo Machinery Department.

### 2.1 Nickel- and Cobalt-Base Alloys

The usefulness of nickel-base alloys is limited by their oxidation resistance and melting point since typical solidus temperatures are 2190° to 2370°F. There is not much more to come from conventional methods of achieving high temperature strength in wrought alloys, viz., by a combination of solid solution strengthening and precipitation hardening, using vacuum melting techniques, particularly as hot working becomes increasingly difficult with more extensive alloying.

Dispersion strengthening, by which finely dispersed particles confine the movement of dislocations, is more attractive than precipitation hardening for retaining strength at higher temperatures. Nickel dispersion hardened with alumina or thoria has the same melting point as pure nickel, and its tensile and creep/rupture strength properties show less tendency to diminish with increasing temperature than conventional super alloys. As far as rotor blading is concerned, however, materials of the TD nickel type serve as models to illustrate the possibilities of such strengthening mechanisms. Higher strength levels and improved oxidation resistance, particularly in the presence of sulphur-bearing gases, are needed, but may be difficult to achieve without affecting the stability of the dispersed phase and without incurring appreciable reduction in melting point.

Castnickel-based alloys have been developed with as much as 120°F advantage over wrought alloys, when comparing the temperatures at which a 100-hr rupture strength of 8 tons/sq. in. is obtained. The stress-to-rupture properties evaluated at the NGTE of some commercially available United Kingdom alloys (see Appendix A) are shown in Fig. 1. Although casting alloys have not reached the limit of their development, strengthening is obtained most readily by addition of heavy metals such as tungsten; and the gain in specific strength is not as attractive as that indicated by laboratory stress/rupture data. In general, a better blend of castability, fatigue, and impact strength (their relative importance is a function of component geometry and engine characteristics) is required and may not be achieved without some sacrifice of creep/rupture strength. Also, the relatively lowly stressed regions near the tip of a rotor blade tend to be those with the highest temperatures, which are approaching currently the limit of oxidation resistance of nickel-base alloys. Certainly, protective coatings will be necessary to prevent excessive intergranular corrosion in the presence of sulfurous gases, particularly as the most recent experimental alloys are low in chromium content.

It is difficult to predict whether cobalt-base alloys can be developed with better properties than nickel-base. No marked superiority in creep strength is expected, but secon-

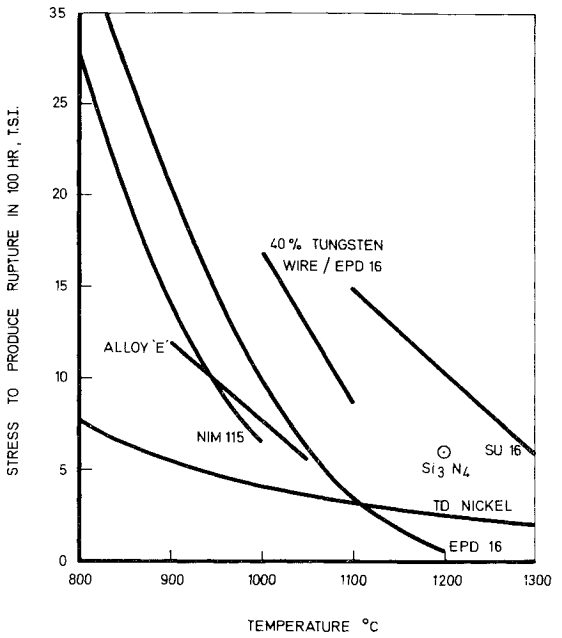


**Fig. 1 100-hr creep rupture strengths.**

dary advantages such as better corrosion resistance may be revealed.

### 2.2 Chromium-Base Alloys

The good oxidation resistance, high melting point (~3450°F), and low density (7.1 g/cm³) of chromium have encouraged metallurgists, particularly those in the Australian Department of Supply, to conduct research on chromium alloys. Considerable progress has been made. Recently, an extensive evaluation of the Australian-developed alloy E (see Appendix A) has been completed at the NGTE. As indicated in Table 1, the creep/rupture properties of specimens of this alloy, made and processed partly or wholly in the United Kingdom and possessing a fully recrystallized structure, are significantly superior to Nimonic 115 but inferior to the best experimental nickel-base casting alloy. On the other hand, the rupture strength evaluated at NGTE of the same alloy processed in Australia and having a "banded" cold-worked structure is superior to typical nickel-base alloys. In common with most wrought alloys, the rupture lives at and above 1830°F are associated with high elongations at fracture. For the rotor blade application, the test durations at 1 and 5% strain, as given in Table 1, are more meaningful. For the same centrifugal loading, the 5% creep and rupture strengths of the Australian-processed alloy E are about 25% greater at 1830°F than the cast nickel-base alloy EPD16.

Using a modified Charpy test, the brittle/ductile transition temperature of the fully recrystallized material was between 570° and 750°F on unnotched, and between 930° and 1020°F on notched specimens. The insensitivity to notches above 930°F (500°C) is destroyed by prolonged exposure at 1830°F in air, i.e., by nitrogen embrittlement. As expected, the oxidation resistance of this alloy in air and in sulphur-bearing atmospheres was adequate at 1830° and 2010°F. Its thermal fatigue resistance, based on the endurances to the first-observed crack, was superior to any nickel-base alloy; but crack propagation rates were very rapid. Evidently, any advances in high temperature strength must be accompanied by improved resistance to nitrogen embrittlement.

### 2.3 Niobium-Base Alloys

Relative to the other refractory metals, the low density (8.57 g/cm³) of niobium, its low brittle/ductile transition temperature, and the refractoriness of its oxide are attractive, while its melting point (4440°F) is sufficiently high to indicate the promise of considerably better high temperature strength properties than nickel- or chromium-base alloys.

The rupture stress/temperature characteristic of the British niobium alloy SU16 shows (see Fig. 1) that this promise has been fulfilled. Although the oxidation resistance of alloys so far developed is considerably better than that of pure niobium, protection is essential for turbine blading. The future acceptability of niobium alloys for service in turbojet engines will depend on the development of suitable protective coatings. The coating composition and technique are likely to vary with the alloy and with the service conditions associated with particular applications. In general, the coating, including the interface region, should be sufficiently refractory, and should retain its integrity under the operating conditions without affecting significantly the strength properties of the

**Table 1 Creep and rupture data on potentially useful turbine blade materials**

| Material | Stress, tons/in.² | Factored[a] stress, tons/in.² | Temp, °F | Hours to 1% strain | Hours to 5% strain | Hours to Rupture | % elongation at rupture |
|---|---|---|---|---|---|---|---|
| Chromium alloy E (cold worked) | 8 | 8.55 | 1830 | 43 | 207 | 445 | 16.1 |
| | 8 | 8.55 | 1830 | 46 | 390 | 608 | 17.2 |
| | 8 | 8.55 | 1830 | 62 | 490 | 824 | 21.7 |
| | 8 | 8.55 | 1830 | 87 | 615 | 963 | 21.0 |
| Chromium alloy E (fully recrystallized) | 6 | 6.4 | 1830 | 138 | ... | 244 | 2.1 |
| | 7 | 7.5 | 1830 | 92 | ... | 197 | 6.0 |
| | 7 | 7.5 | 1830 | 89 | ... | 140 | 6.0 |
| | 8 | 8.55 | 1830 | 20 | ... | 61 | 3.6 |
| Nickel alloys: | | | | | | | |
| Nimonic 115 (wrought) | 8 | 8 | 1830 | 5 | 23 | 28.5 | 17.1 |
| EPD 16 (cast) | 7 | 6.45 | 1830 | ... | 536 | 550 | 8.1 |
| | 8.5 | 7.8 | 1830 | 118 | ... | 177 | 3.7 |
| EPK 36 (cast) | 7 | 7 | 1830 | 45 | ... | 243 | 3.3 |
| | 8 | 8 | 1830 | 46 | ... | 113 | 4.2 |
| Niobium alloys: | | | | | | | |
| Alloy F[b] | 10 | 8.35 | 2010 | 100 | 237 | [c] | ... |
| | 15.5 | 12.9 | 2010 | ... | ... | 97.5 | 14.7 |
| SU16[b] | 10 | 8.4 | 2010 | 100 | ... | ... | ... |
| | 8 | 6.75 | 2100 | 97 | ... | ... | ... |

[a] Factored stress = test stress × density of Nimonic 115/density of alloy.
[b] Protected with NGTE coating.
[c] UB = unbroken.

niobium alloy. Thus, metallurgical stability, i.e., freedom from phase transformation and excessive inter-diffusion with the substrate, is essential; if the coating is brittle, its thermal expansion characteristics should match closely those of the substrate. In particular, an acceptable level of resistance to foreign body damage is essential. Despite the protective virtues of silicides, it appears unlikely that a single-phase coating will possess all the desired characteristics.

Laboratory tests at NGTE on the two niobium alloys, F and SU16 (see Appendix A for compositions), protected by a two-phase "composite" coating, indicate that their resistance to cyclic oxidation is good, as Table 2 shows. The creep and stress-to-rupture characteristics are essentially the same as for the unprotected alloy. For the same centrifugal loadings, the data in Table 1 indicate that, at stresses of ~8 tons/sq. in., protected niobium alloys have at least a 200° temperature advantage over cast nickel-base alloys and chromium alloy E. The brittle/ductile transition (Charpy test) of the coated alloy is below room temperature; thus, foreign body damage may fracture the coating locally, but not the substrate. In general, this experimental coating compares favorably with the best commercially available United States coatings evaluated under the same conditions.

### 2.4 Composites

The high strengths and high moduli of whiskers (typically a few microns in diameter) and the high strengths of fine wires, or of ceramic fibers that are free from surface flaws, certainly are attractive for reinforcing metallic matrices. For high temperature applications, the stability of the reinforcement is of paramount importance. Even if whisker integrity is retained during processing, it is unlikely that it will be maintained after exposure for several hundred hours at temperatures above 1830°F. Inter-diffusion tests under such conditions on nickel-base alloys cored with alumina and silicon carbide rods indicate, however, that fibers of ~0.010-in. diam in these materials would be largely unaffected. The development of techniques for making such fibers of this size and for introducing them into the matrix needs greater attention.

Laboratory experiments at NGTE on the reinforcement of nickel-base cast alloys with fine tungsten wires have achieved substantial improvements in creep-rupture strength (see Fig. 1). On specific strength considerations, however, this gain is reduced greatly because of the high density (12.2 g/cm$^3$) of the composite. It is interesting to note that the rupture-strength properties at 1830°K and 2010°F (1000° to 1100°C) of this composite, containing 40% by volume of 0.010-in.-diam tungsten wire, were predictable from the rupture strength data determined for the matrix and for the individual tungsten wires.

### 2.5 Ceramics

The attractions of ceramics, viz., low density, high melting point, high oxidation resistance, and retention of strength at high temperatures, are counter-balanced by their complete absence of ductility which is evident in their very poor resistance to mechanical shock, and also to thermal shock unless their thermal properties are particularly favorable. The low coefficient of expansion of silicon nitride is largely responsible for its good thermal shock characteristics. If the likelihood of chance impact damage were reduced, and if its mechanical properties were more reproducible, silicon nitride could be used for nozzle guide vanes by virtue of its refractoriness (melting point ~3450°F) and excellent oxidation resistance (to ~2730°F). Because of the problems in designing for a fully brittle material, ceramics may well be used first in fiber rather than in bulk form for rotating blades.

**Table 2 Oxidation test data**

| Coating designation | Substrate | Oxidation lifetime at temperature, °F: Cyclic oxidation (Tm–Tr) hr at | | Pest oxidation[a] (Tm–Ti–Tr), No. of cycle |
|---|---|---|---|---|
| Thompson Ramo Wooldridge Inc. Cr–Ti–Si | Alloy F | 2010 or 2190 | 2370 | 2010, 2190, or 2370 |
| | | 100+ | 50 → 100+ | 20+ |
| Sylvania R513 Cr–Ti–Si | Alloy F | 100+ | 100+ | 20+ |
| NGTE coating | Alloy F SU16 | 100+ | 100+ | 20+ |

[a] Pest oxidation cycle = 2 hr Tm, 2 hr Ti, 1 hr Tr. Tm = maximum temperature: 1100°, 1200°, or 1300°C. Ti = intermediate temperature 800°C. Tr = room temperature.

## 3. Internally Cooled Blading

Cooling of turbine blades, using air bled from the compressor delivery and allowing it to flow through passages formed within the blades, is well established as a technique that allows the use of turbine inlet gas temperatures high enough to cause a serious loss of strength, oxidation, and possible melting in uncooled blades. With cooled blades, the gas temperature that can be used depends on the permissible blade temperature, the cooling air supply temperature, and on the internal geometry of the blade which governs both the rate of flow of cooling air for the available pressure drop, and the effectiveness with which heat is transferred from the internal surfaces of the blade to the cooling air.

### 3.1 Nature of the Problem

The specification of a permissible blade temperature depends very much on whether the cooled blade is a stator or a rotor blade (bucket). With stator blades, intense local cooling often is needed at the leading edge at or near the midspan position in order to prevent local oxidation or melting. This requirement is important particularly if the gas stream leaving the combustion chamber has a very nonuniform temperature pattern. Therefore, most of the cooling air is led directly from the supply to the leading edge and then is allowed to pass to the remainder of the blade. High temperatures also may be a problem in the trailing edge, particularly if it is slender. For this reason, and also because it provides a convenient way of discharging spent cooling air into the main stream with a minimum of pressure loss because of mixing, film-cooling is used often. The air is discharged on the concave surface of the blade from a series of slots or holes at or close to the trailing edge.

For a rotor blade, life is governed usually by creep considerations, and because the applied stresses caused by rotation and gas bending effects tend to fall from root to tip, the preferred form of blade temperature distribution is one that rises from root to tip. When cooling air is fed into the root of a rotor blade and flows radially outward through uniform spanwise passages, this form of temperature distribution is achieved. However, it is seldom, if ever, that the stress and temperature distributions match each other along the span of the blade in such a way as to insure that all parts of the span will have the same creep life. It is usual to find the most severe combination of stress and temperature near the mid-span position; experiments with cooled blades subjected to endurance tests have confirmed this.[1,12] Therefore, the cooling performance of the blade at the mid-span can provide a very good guide to the conditions under which it can be operated.

In what follows it will be assumed that rotor blade temperatures and stresses will provide the limit to the permissible turbine inlet gas temperature. Although it is possible to envisage a limit set by oxidation or melting of the first stage stator, where both the maximum and the mean gas temperatures will be higher than those relative to the moving blade, it must be remembered that the cooling air supplied

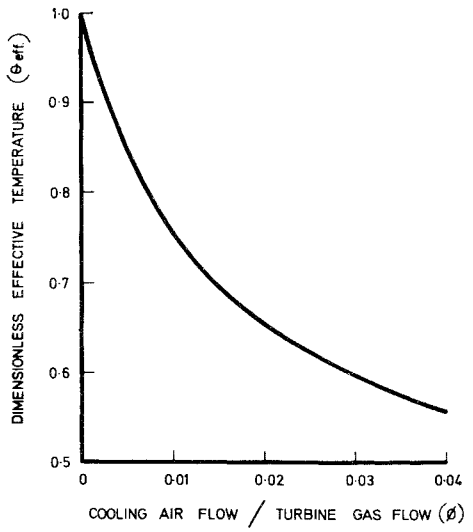


**Fig. 2 Cooling characteristic for rotor blade.**

to the root of the rotor blade usually will be hotter than that supplied to the stator, by virtue of relative speed effects. Also, the aspect ratio of the rotor blades probably will have to be higher than that permitted in the stator blades in order to limit the disk rim stresses and hence the disk weight. This limitation of aspect ratio means smaller chord widths and smaller cross-section areas for the flow of cooling air in the rotor blades when compared with the stator blades. It could necessitate also a simpler and less effective system of cooling passages. The remainder of the discussion therefore will be devoted to the cooling of rotor blades and will deal with the effects of blade material (and hence permissible blade temperature) on gas temperatures in turbojet and by-pass engines at cruise conditions of $M = 2.2$ in the stratosphere. In all the examples investigated, the over-all compressor pressure ratio has been assumed to be 8, and the cooling air supply temperature has been taken as 1500°R (820°K).

### *3.1.1. Effects of thermal stress*

Although examination of the chordwise mean temperatures and centrifugal stresses along the span provides a good guide to the most severely loaded part of a blade, any estimate of blade life, using a rupture or a specified creep strain criterion, would be misleading if based simply on this temperature and stress. The influence of chordwise variations of temperature have to be taken into account. They occur because lack of space for cooling passages, together with high local values of heat transfer coefficient at the leading and trailing edges, usually cause these parts of a blade to run hotter than the remainder. The distribution of stresses acting in the spanwise direction is nonuniform therefore over a chordwise section, with the highest values of tensile stress in the mid-chord region and the smallest values at the leading and trailing edges. This stress pattern is the result of a redistribution process caused by creep. With a perfectly elastic material, the thermal stresses in the hottest parts of a blade could well exceed the centrifugal tensile stress at the midspan position, thereby causing the local net stresses to be compressive, whereas the maximum tensile stresses in the mid-chord region would be much larger than the redistributed values, perhaps by a factor of 2. It has been shown[3] that a predicted blade life based on the redistributed stress pattern and the associated temperatures is significantly smaller than the life based on the centrifugal stress and the chordwise mean temperature. Conversely, if the centrifugal stress is to be used to predict blade life from creep data for the blade material, it must be used in conjunction with a temperature somewhat higher than the chordwise mean value at midspan.

It is reasonable to expect the difference between this effective temperature and the mean temperature to depend on the uniformity of the temperature distribution across the chord. It is reasonable also to expect this nonuniformity to become more marked progressively as the degree of cooling is increased in a given blade. A dimensionless blade temperature, which varies with cooling flow, therefore has been defined; and an arbitrary relationship is proposed between the effective value of this parameter for life estimation purposes and the mean value based on actual metal temperatures. The dimensionless blade temperature $\theta$ is defined[4] as

$$\theta = (T_b - T_c)/(T_g - T_c)$$

where $T_b$ is the blade temperature, $T_c$ is the cooling air temperature in the blade root, and $T_{g(\mathrm{rel})}$ is the mean gas temperature relative to the moving blade. The arbitrary relationship proposed between the dimensionless effective temperature $\theta_{\mathrm{eff}}$ and the mean value $\bar{\theta}$ is

$$1 - \theta_{\mathrm{eff}} = k(1 - \bar{\theta})$$

Evidence for a value of the factor $k$ is scanty at present. The unpublished results of stress redistribution calculations at NGTE on an experimental blade indicated values close to 0.84 for three different blade alloys. However, with a midspan $\bar{\theta}$ of 0.75, the maximum value of $\theta$ at the trailing edge was 0.83, which is rather lower than might be expected with an engine blade having the same $\bar{\theta}$, with a more slender trailing edge and less space for cooling passages. For this reason, and also to provide some allowance for radial gas temperature

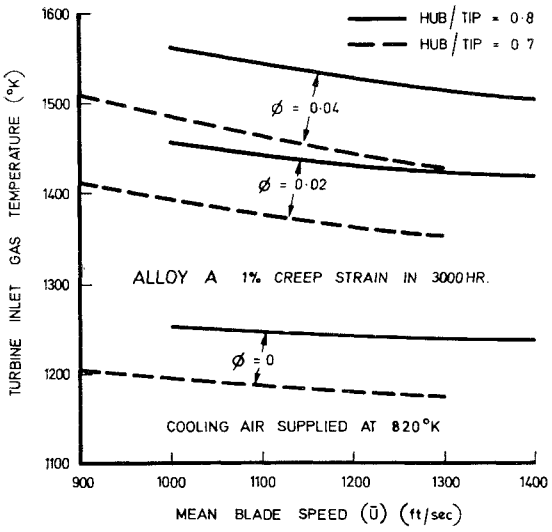


**Fig. 3 Permissible turbine inlet temperature (alloy A).**

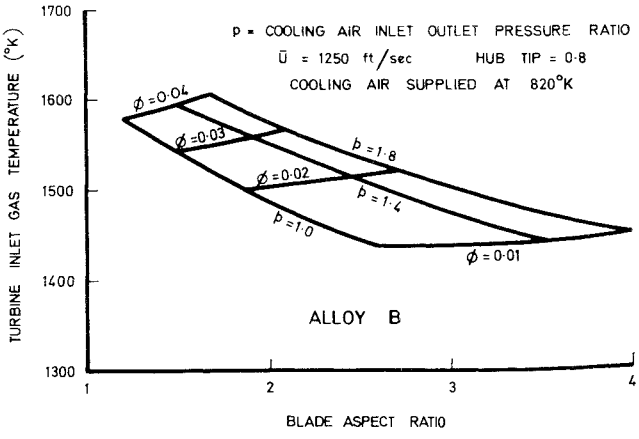


**Fig. 4 Effects of aspect ratio and pressure drop.**

profiles having their maximum values at or near the midspan region, a value of 0.75 was chosen for the factor.

#### 3.1.2. *Permissible turbine inlet temperatures*

The values of $\bar{\theta}$ and $\theta_{\text{eff}}$ will depend on the blade geometry, the external gas flow conditions, and the ratio of the cooling airflow to the turbine gas flow ($\phi$). A typical calculated curve of $\theta_{\text{eff}}$ vs $\phi$ is shown in Fig. 2. It is known to be representative of blades with good internal heat-transfer characteristics and has been used as a basis for estimating permissible turbine gas inlet temperatures over a range of mean blade speeds and hub/tip ratios for two different alloys. The results are shown in Fig. 3 for a hypothetical alloy A, typical of the best nickel-base casting alloys currently available, and in Fig. 4 for another, alloy B, assumed to have the same density and the same 3000 hr/1% creep strength at a temperature 110°F (50°C) higher than the value for alloy A.

The flatness of the curves with increasing blade speed may seem surprising at first sight. However, it must be remembered that, for a given set of turbine flow angles, the difference between the mean gas inlet stagnation temperature and the mean gas temperature relative to the moving blades is proportional to the square of the mean blade speed. This has been allowed for in converting the relative temperatures to inlet temperatures. (Details are given in Appendix B.)

The permissible blade temperatures at $\phi = 0.02$ and 0.04 were obtained from stresses computed at the midspan position and were converted to gas relative temperatures assuming the curve of $\theta_{\text{eff}}$ in Fig. 2. The basic supply temperature of 1475°R for the cooling air was increased by a correction to allow for relative speed effects. The temperatures for $\phi = 0$, i.e., uncooled blades, were obtained from stresses computed at one-third of the blade height from the root. The presence of nonuniform gas temperature profiles in the radial sense, together with some cooling by spanwise conduction near the root, have tended to transfer the most critical region of an uncooled blade from the root itself to the one-third height.

Because of the relatively high cooling air supply temperature, a cooling flow ratio of 0.04 is needed to make a turbine inlet temperature of 2700°R (1500°K) feasible with cooled blades cast in alloy A. By contrast, a 110°F improvement in blade properties can lead nearly to 210° rise in permissible turbine inlet temperature with $\phi = 0.04$ or (more likely) a reduction in $\phi$ to 0.02 in order to achieve 2700°R. Either way, the importance of improved materials is emphasized.

#### 3.1.3. *Turbine design*

Having indicated what can be achieved with cooling flow ratios up to 0.04, it is of interest to examine the way in which turbine design may be influenced by such a requirement. This has been done for alloy B with a mean blade speed of 1250 fps and a hub/tip ratio of 0.8, and is illustrated in Fig. 4 in terms of blade aspect ratio and the pressure ratio available to pass the coolant through the blades. As the blade aspect ratio was changed, the cooling passage configuration was kept the same by maintaining constant values of passage flow area/chord$^2$ and passage perimeter/chord (see Appendix B). This pitch/chord ratio was maintained constant also, so that the number of blades increased proportionately with the aspect ratio. The net result is that for a given coolant pressure ratio the permissible flow and hence the permissible turbine inlet gas temperature both fall as the aspect ratio is increased. For a cooling system of the kind considered, where the cooling air is fed to the blade roots at a pressure only slightly below that of the compressor delivery and is exhausted at the tip of a shrouded blade to a static pressure close to that immediately downstream of the stage, practical values of cooling air pressure ratio will lie between 1.4 and 1.8. However, results for a pressure ratio of 1, when the pumping action of the blades provides the sole means of overcoming friction and heating pressure losses, have been included because they show the penalty to be paid by pressure losses in the cooling air supply and by tip leakage effects, which raise the pressure at exit from the cooling passages. For a blade with an aspect ratio of 3, capable of operating at a turbine inlet temperature of 2700°R (1500°K) when the cooling pressure ratio is 1.8, a reduction to 2655°R (1475°K) is necessary to maintain the same blade life if the coolant pressure ratio falls to 1.4. The temperature will have to be reduced still further to 2590°R (1440°K) at a pressure ratio of 1.2.

The corresponding curves for alloy A would be very similar, but would, of course, indicate lower turbine inlet temperatures at a given aspect ratio and pressure ratio. In particular, the temperature of 2700°R, attainable with an aspect ratio of 3 using alloy B, would demand an aspect ratio of less than 2 in order to allow blades made from alloy A to pass the required cooling flow. This would involve a direct penalty in turbine weight, both from the increased blade weight and from the thicker disk needed to support them. It would probably involve also some penalty in turbine aerodynamic performance, although this is unlikely to be important under supersonic cruise conditions. The only point in favour of a blade in which a small aspect ratio is necessary is that the resultant increase in chord length and cross-section area probably would make it possible to use a more efficient system of cooling passages, thereby leading to some saving in cooling air requirements. Because of the associated increase in pressure loss characteristics, it is unlikely to permit any worthwhile increase in turbine inlet temperature.

#### 3.1.4. *Engine performance*

Throughout the preceding discussion of the characteristics of internally cooled blades, it has become apparent that any improvement in materials, leading to an increase in permissible blade temperature for a given stress and life, is likely to have a very strong influence on engine design. Because of the relatively high temperature of the cooling air in the supersonic engine application, it has become necessary to consider blades capable of operating at effective dimensionless temperatures of 0.6 or even less. On this basis, a 110°F improvement in permissible blade temperature can be regarded as allowing an increase of over 80° in the turbine inlet temperature. A more probable alternative, because of the temperature limitations imposed by oxidation, is that it allows a significant reduction in turbine weight and in the cooling flow requirement. Whichever way the improvement is used, it is of interest to see the effect on engine performance. The example chosen for illustration is a series of design points for bypass engines in which the over-all pressure ratio of 8 and the bypass ratio of 1 are maintained constant as the turbine entry temperature is raised. Downstream of the turbine the main engine flow and the bypass flow are assumed to be mixed fully so the pressure ratio of the low pressure compressor is allowed to increase as the turbine inlet temperature is raised.

If no blade cooling were required, a very rapid rise in specific thrust could be achieved, as can be seen from curve 3 in Fig. 5. The effect of having to bleed cooling air for the turbine blades from the compressor delivery is to cause a loss of specific thrust at a given turbine inlet temperature, as would be expected. The effects are less marked on thrust work efficiency, which is defined as the product of the thrust and flight speed divided by the product of the fuel flow and the calorific value of the fuel, using consistent units. The curve marked 1 applies to a turbine needing no blade cooling air at an inlet temperature of 2340°R (1300°K). Reference to Fig. 6 shows that this in itself would demand a rotor blade material such as alloy B. The progressively larger demands for cooling air as the turbine inlet temperature is increased

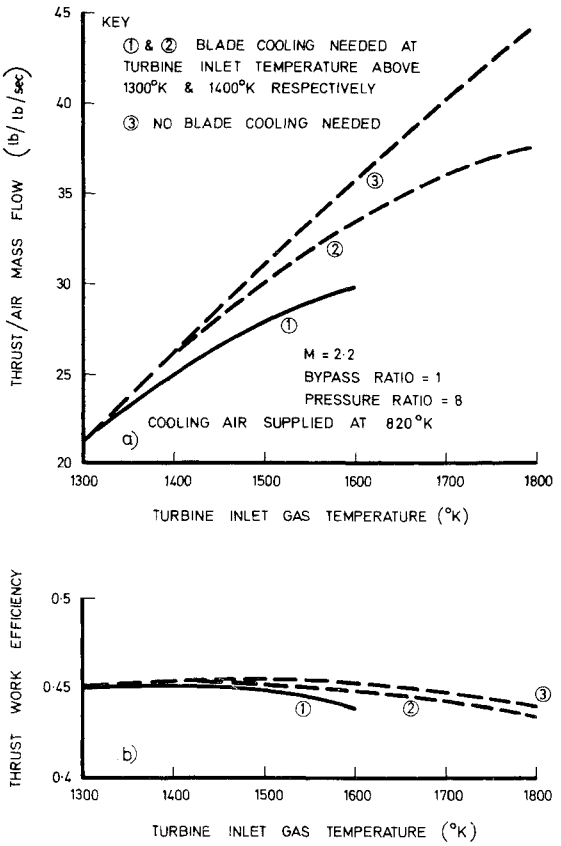


**Fig. 5 By-pass engine performance.**

result in a flattening of the specific thrust curve, and at temperatures above 1600°K it is clear that there is likely to be no worthwhile improvement in specific thrust, even if blades could be designed to pass the required cooling flows.

The curve marked 2, applying to a turbine needing no cooling air at an inlet temperature of 2520°R, shows what might be achieved in the more distant future, and once again emphasises the importance of advances in the technology of turbine blade marerials.

### 3.2. Effect of Technique of Producing Cooling Passages on Material Properties

Cooling passages can be produced in turbine blades by several techniques that modify to different degrees the micro-

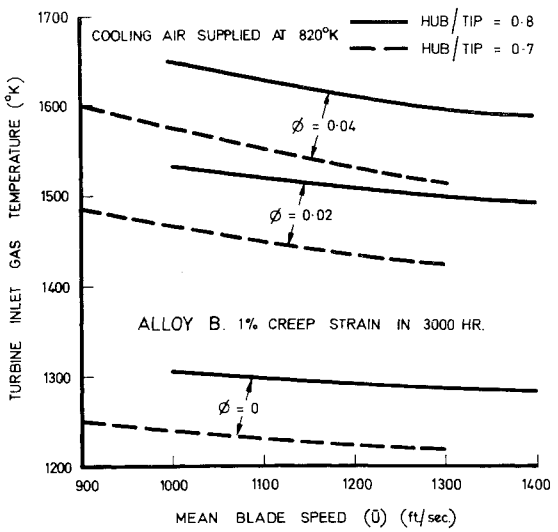


**Fig. 6 Permissible turbine inlet temperature (alloy B).**

**Table 3 Influence of hole-forming process on creep and fatigue properties of nickel-base alloy**

| | % reduction in 100-hr rupture strength | | | | |
|---|---|---|---|---|---|
| | Creep-rupture | | Fatigue ($12 \times 10^6$ cycles) | | |
| Type of test piece | 1500°F | 1650°F | 1500°F, 0 ± P | 1500°F, P ± 0.25P | 1650°F, 0 ±P |
| Hole-free (extruded) | 0 | 0 | 0 | 0 | 0 |
| Holes produced by: | | | | | |
| Extrusion technique | 13 | 19 | 10 | 11 | 15 |
| Spark-erosion | 13 | 22 | 16.5 | 33 | 8 |
| Mechanical drilling | 9 | 7.5 | 18 | 30 | 6 |
| Electro-chemical drilling | 17 | 22 | 51 | ... | ... |
| Hole-free (vacuum cast) | 0 | 0 | 0 | ... | 0 |
| Holes produced by casting technique | 7.5 | 6.5 | 0 | ... | 5 |
| Hole-free (sintered) | 0 | 0 | 0 | ... | ... |
| Holes produced by sintering technique | 14 | 22 | 33 | ... | ... |

structure surrounding each passage. The presence of residual stresses, local coarsening of the grain size or recrystallization (during the hole-forming process or by subsequent heat treatment), and intergranular cracking may affect detrimentally the creep and fatigue properties of the blade. The extent of the effects was determined by conducting comparative tensile creep and push-pull fatigue tests on specimens with and without cooling passages (see Fig. 7) in material of the same nominal composition (alloy X, Appendix A) prepared by extrusion, vacuum-casting, and sintering techniques, respectively. The filler or core material used to produce the circular section holes was removed by volatilization during processing (sintered specimens) or by subsequent leaching (extruded and cast specimens). (For the investment-cast specimens, fused silica tube cores were used and removed from the castings by molten caustic soda, a technique first developed at NGTE over 15 years ago for the manufacture

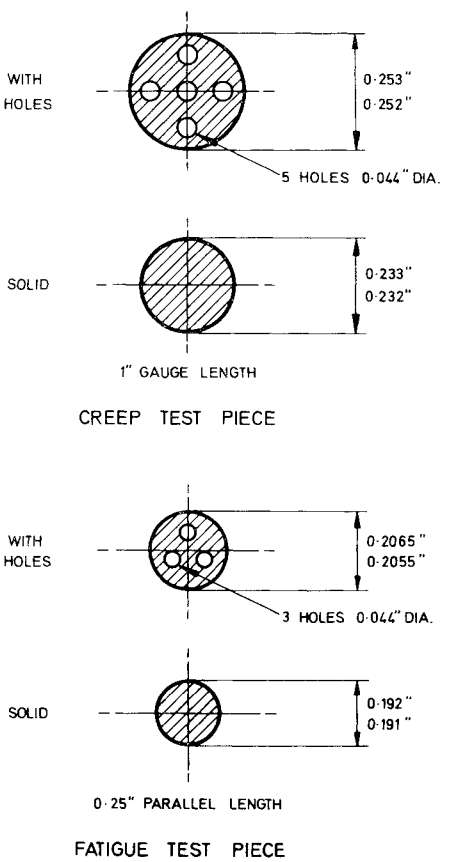


**Fig. 7 Test pieces for cooling hole investigation.**

of cooled blades.) Prior to machining, the specimens were fully heat-treated, viz., solution treated for 8 hr at 1975°F and aged for 16 hr at 1240°F. Holes were produced also in heat-treated extruded bar by spark-erosion, mechanical drilling, and electro-machining, respectively. In all cases, the hole-free specimens had the same cross-sectional area of solid material as the specimens containing holes.

The test data (see Table 3) showed that the extent of the deterioration incurred by each hole-forming process varied with the life. Nevertheless, the reduction in the 100-hr creep/rupture and fatigue strengths was reasonably typical of each process. Assuming the absence of stress concentrations associated with the geometry of the cooling passages, the casting process produced the least deterioration in properties. Metallographic examination showed that all other processes had produced significant changes in the microstructure of the hole walls, particularly in the case of the extruded holes where integranular fissures arising from penetration of the filler metal during extrusion were evident. Naturally, it is possible to minimize such effects in all processes, but the investigation served to indicate that the acceptability of a production technique must be assessed not simply on the ease of hole-forming but on the degree of freedom from deleterious effects on the material of the hole walls.

## 4. Conclusions

The preceding sections have served to emphasize the way in which both improved alloys and the use of internally cooled blades together can permit high turbine inlet gas temperatures during supersonic cruising flight. Without the improved alloys, the extent to which cooling by itself can allow increased gas temperatures is limited principally by the relatively high temperature of the cooling air, which leads to a requirement for comparatively large cooling flows and hence for blades of low aspect ratio.

Although materials good enough to permit turbine inlet gas temperatures as high as 2700°R without the use of internal cooling may ultimately by developed, the requirement for some degree of internal cooling is likely to remain for a long time to come. For this reason, the need for materials capable of redistributing thermal stresses with little or no adverse effect on blade life and the effects of hole-forming processes on the creep and fatigue properties will remain an important consideration.

## Appendix A: Composition of Alloys

**Table 4 Nominal percentage composition**

| Alloy | C | Si | Cr | Ti | Al | Co | Mo | Ni | Nb | Ta | W | B | Zr |
|---|---|---|---|---|---|---|---|---|---|---|---|---|---|
| Ni-base alloys | | | | | | | | | | | | | |
| Alloy X | 0.10 | ... | 20 | 2.4 | 1.2 | 20.0 | ... | Bal. | ... | ... | ... | ... | ... |
| Nimonic 115[a] | 0.15 | ... | 15.0 | 4.0 | 5.0 | 15.0 | 3.5 | Bal. | ... | ... | ... | ... | ... |
| EPD 16[a] | 0.12 | ... | 6.0 | | 6.0 | ... | 20 | Bal. | 1.5 | ... | 11.0 | 0.02 | 0.12 |
| EPK 36[a] | 0.10 | ... | 10.0 | 5.0 | 5.0 | 10.0 | 4.0 | Bal. | ... | ... | ... | 0.015 | 0.12 |
| T.D. nickel | ... | ... | 2% thoria | | ... | ... | ... | Bal. | ... | ... | ... | ... | ... |
| Cr-base alloys | | | | | | | | | | | | | |
| Alloy E | 0.01 | 0.5 | Bal. | 0.1 | ... | ... | ... | ... | ... | 2 | ... | ... | ... |
| Nb-base alloys | | | | | | | | | | | | | |
| Alloy F[b] | 0.03 | ... | ... | ... | ... | ... | 5.0 | ... | Bal. | ... | 15 | ... | 1 |
| SU16[b] | 0.08 | ... | ... | ... | ... | ... | 2.0 | ... | Bal. | ... | 21 | ... | ... |

[a] Supplied by Henry Wiggin and Co. Ltd., Birmingham, England.
[b] Supplied by I.M.I. Ltd., Witton, Birmingham, England.

## Appendix B: Assumptions Used in the Calculation of Turbine Inlet Gas Temperature and Blade Cooling

### Turbine Inlet Gas Temperature

At a given mean blade speed $U$, the difference between the mean gas total temperatures at the turbine inlet ($T_{t_0}$) and relative to the moving blades ($T_{t_1}$) depends on the aerodynamic characteristics of the turbine stage, typified by the aerodynamic loading factor ($\Delta H/U^2$), the degree of reaction, and the flow coefficients at inlet to and outlet from the rotor blades. For the turbine stage under consideration, the following were assumed:

$$\Delta H/U^2 = 1.5 \qquad \text{Reaction} = 50\%$$

$$\text{Flow coefficient} = 0.75 \text{ at inlet and outlet}$$

These parameters are regarded as typical of a turbine stage of high isentropic efficiency. They also result in a symmetrical velocity diagram so that

$$T_{t_0} - T_{t_1} = 0.75\ U^2/k_p$$

where $k_p$ is the appropriate value of specific heat at constant pressure.

Now, consideration of the midspan stress at a given mean blade speed and hub/tip ratio, together with the required life and the creep properties of the blade material, gives a permissible blade temperature. For a specified cooling air supply temperature and a chosen internal geometry, a corresponding gas relative temperature $T_{g(\text{rel})}$ can be deduced. Although $T_{g(\text{rel})}$ is less than $T_{t_1}$ because of a recovery factor slightly less than unity, it is a reasonable approximation to assume $T_{t_1} = T_{g(\text{rel})}$ for the purpose of these calculations. This leads to deduced values of the mean gas inlet temperature which are about 18° R lower than would be the case otherwise.

### Blade Cooling

For the results shown in Fig. 5, the blade internal geometry was such that

$$\text{flow cross-section area/chord}^2 = 0.021$$

$$\text{wetted perimeter/chord} = 2.82$$

These combine to give a $Z$ factor (defined in Ref. 3) of 165 and could be achieved, for example, in a blade of a 1.5-in. chord by having 13 passages of elliptical cross section, with major and minor axes equal to 0.15 in. and 0.03 in., respectively.

The pitch/chord ratio was taken as 0.7 and, for the turbine stage parameters given previously, the gas outlet angle rela-

tive to the rotor blade, measured from the axial direction, was 59°.

The curve of effective relative temperature given on Fig. 2 was based also on this geometry, and applies for an aspect ratio of 2 and a gas Reynolds number of $6 \times 10^5$, based on blade chord and relative gas conditions at exit from the rotor blade row.

## References

[1] Barnes, J. F. and Fray, D. E., "Some aspects of research at the National Gas Turbine Establishment on internally air-cooled turbine blades," Institution of Mechanical Engineers, Thermodynamics and Fluid Mechanics Convention Paper 4 (April 1964).

[2] Hare, A. and Malley, H. H., "Cooling modern aero-engine turbine blades and vanes," Society of Automotive Engineers Paper 660053 (January 1966).

[3] Barnes, J. F. and Clarke, J. M., "The significance of creep in cooled gas turbine blades," Proc. Inst. Mech. Engrs. **178**, Pt. 3L (1963–1964).

[4] Ainley, D. G., "Internal air cooling for turbine blades: A general design survey," British Aeronautical Research Council R & M 3013 (1957).